

非晶矽/單晶矽吸光區累崩區分離 累崩光二極體特性

施能夫

摘要

本研究以一個雙載子積體電路相容的製程來製作非晶矽/單晶矽吸光區累崩區分離累崩光二極體(SAM-APD)。爲了避免元件製作時參數錯誤所造成試錯誤的時間浪費，在設計元件時先以元件模擬軟體及製程模擬軟體來模擬製造時所需要的參數。單晶矽的電子對電洞碰撞游離率比值遠大於1，而非晶質矽於可見光的光吸收係數十分恰當，這兩種材質的合併可導致高增益低雜訊的累崩光二極體。由於複雜的製程及未求最佳化，目前所得到的光增益爲3.4。

關鍵字：非晶質、異質介面、雙載子、電晶體。

Characteristics of Amorphous Silicon/Crystalline Silicon Separated Absorption Multiplication Avalanche Photodiode (SAM-APD)

Neng-Fu Shih

Abstract

A BJT compatible process was used to fabricate an amorphous/crystalline Si separated absorption multiplication avalanche photodiode (SAM-APD) in this study. In order to avoid the wasting time of try and error, using the device simulator and the process simulator simulated the performance and the process parameters of the designed SAM-APD's. The ratio of electron and hole ionization coefficient in crystalline Si is largely different from unity, which will result in low excess noise factor. The absorption coefficient for amorphous Si is appropriate in visible light. The combination of these advantages results in high gain low noise avalanche photodiode. Due to process complexity and non-optimum condition, the maximum optical gain of the proposed SAM-APD is 3.4..

Key Words : amorphous, heterojunction, bipolar, transistor °

1. Introduction

Very low noise operation at high gain is a desirable requirement for photodetectors in optical communication systems. The photomultiplier tube provides the highest gain at lowest noise of any existing photodetector. However, due to its large size, high-voltage requirements, and after pulsing [1], its usefulness is limited.

Alternatively, through carrier multiplication in semiconductor materials, avalanche photodiodes (APD's) provide gain. In photodetection applications that require high gain at low noise, these microstructure devices are used widely because these can be easily integrated. Especially, APD's are used widely as detectors in fiber-optic communication systems. The potential advantages of APD's as detectors for optical communication systems have been well established.

As demonstrated by McIntyre [2], low excess noise can be obtained in an avalanche photodiode when the electron and hole impact ionization differ greatly. However, most III-V semiconductors have

nearly equal electron and hole ionization coefficients [3,4].

The quantum efficiency of separated absorption and multiplication layer avalanche photodiode (SAM-APD) is determined by the properties of the absorption layer and the hetero-interface, while the avalanche multiplication process in the multiplication region determines the multiplication and excess noise properties.

When the SAM-APD idea is exported to silicon, it has following advantages: The ratio of electron and hole ionization coefficient in Si is largely different from unity, which will result in low excess noise factor. The absorption efficiency of amorphous silicon (a-Si) for the visible light is at least one order of magnitude higher compared to crystalline silicon. Additionally amorphous materials have a very low deposition temperature (when PECVD system is used), and are easy to be deposited onto any substrate without the problem of lattice mismatch, and do not contain any material harmful to Si IC's fabrication processing.

2. Fabrication of the sam-apd's

Fig. 1 shows the schematic cross-section of the proposed SAM-APD. In order to save the time of try and error in all process, all process parameters are determined from the simulation result. An Avant's process simulation software - TSUPREM4 was used to simulate the fabrication process to check the device doping profile and the design rule. The simulated doping profile was used as the input file of the two dimensional device simulator, to check the breakdown voltage, and currents etc. An Avant's two dimensional device simulator- Medici was used by using a concentration dependent mobility model for the crystalline silicon [5] together with a parallel field dependent mobility model which allows for carrier velocity saturation at high electric fields. Band gap narrowing in the crystalline silicon at a high doping was accounted for. Shockley-read-Hall recombination with concentration dependent lifetimes and Auger recombination models were also included. A detailed physical model of a-

Si:H is incorporated into the simulator to examine the current gain limits of SAM-APD's. After deciding the doping concentration and thickness of each layer, the parameter used in TSUPREM 4 was used as the process parameters, i.e., the thermal temperature, gas flow rate etc..

A <100> orientation with p-type doping level of $1 \times 10^{15} \text{cm}^{-3}$ silicon wafer was used as substrate. The substrate was put into a high temperature furnace to form a 400 nm thick SiO_2 after standard RCA cleaning. The oxidation temperature was kept at 1050°C with $\text{H}_2=3\text{slm}$ and $\text{O}_2=4.8\text{slm}$ for 36 minutes. After photolithography, As bury layer pattern was formed through a medium-energy ion implanter. The implantation energy and dosage are 75KeV and $3 \times 10^{15} \text{cm}^{-2}$, respectively. The drive in condition is 1150°C for 2 hours with $\text{N}_2=8\text{slm}$ and followed by 1050°C oxidation with $\text{H}_2=4.8\text{slm}$ and $\text{O}_2=3\text{slm}$ for 36 minutes. After photolithography, a BF_2 dopant with a doping level of $2 \times 10^{14} \text{cm}^{-2}$ was implanted into the wafer and followed by 1150°C

drive in to form a down-isolation region in an O_2 ambient. After drive in and SiO_2 removal, the bury layer junction depth is around $4.0 \mu m$.

The wafer was put into an epitaxy reactor to form a $5 \mu m$ thick $0.95 \Omega\text{-cm}$ epitaxy layer, i.e. phosphorus doping level of $3 \times 10^{16} \text{cm}^{-3}$ since the goal of breakdown voltage is around 30 volts. The deposition rate is about $1.2 \mu m/\text{min}$, and the operating temperature is 1150°C . After standard RCA cleaning, the substrate was put into a high temperature furnace to form a 400nm thick SiO_2 . After photolithography, a $2 \times 10^{14} \text{cm}^{-2}$ BF_2 was implanted into the wafer and followed by 1150°C driving in to form a top-isolation region in an O_2 ambient. In order to reduce collector series resistance, a deep N^+ region was formed after the photolithography. The implantation energy and dosage are 75KeV and $3 \times 10^{15} \text{cm}^{-2}$, respectively. The p^+ -regions was form though BF_2 implanting with dose level of $3 \times 10^{15} \text{cm}^{-2}$. In order to avoid P^+ -regions over driving, a 200\AA undoped amorphous silicon dioxide was

deposited by the use of a plasma-enhanced chemical vapor deposition (PECVD, ULVAC CPD-1108D) system and followed by a 950°C drive in to get a p^+ -regions with a junction depth of $1.5 \mu m$. After opening the contact holes on p^+ -regions, a 250\AA p^+ -a-Si:H / 3000\AA i-a-Si:H films and a 2000\AA ITO film were deposited by using a PECVD system and a sputtering (ULVAC RFS-200) system, respectively. The flow rate of SiH_4 , operating temperature, pressure, and rf power during deposition of i-a-Si:H are 100sccm , 180°C , 0.25 torr , and 20W , respectively. The flow rate of 4% SiH_4 diluted in H_2 , 1% B_2H_6 diluted in H_2 , operating temperature, pressure, and rf power during deposition of p^+ a-Si:H are 100sccm , 36sccm , 180°C , 0.3 torr , and 10W , respectively. The optical gaps of p^+ -a-Si:H and i-a-Si:H films are 1.68 eV and 1.92 eV , individually. Where using lift-off technique formed the p^+ -i-a-Si:H and ITO regions. A 3000\AA Al film was deposited with an E-beam coater after opening the contact holes on N^+ -regions. Defining the electrode

pattern of ITO and N⁺-regions, then the Al electrodes were annealed in

hydrogen gas at 400°C for 10 min. to alloy the Al in the contact holes.

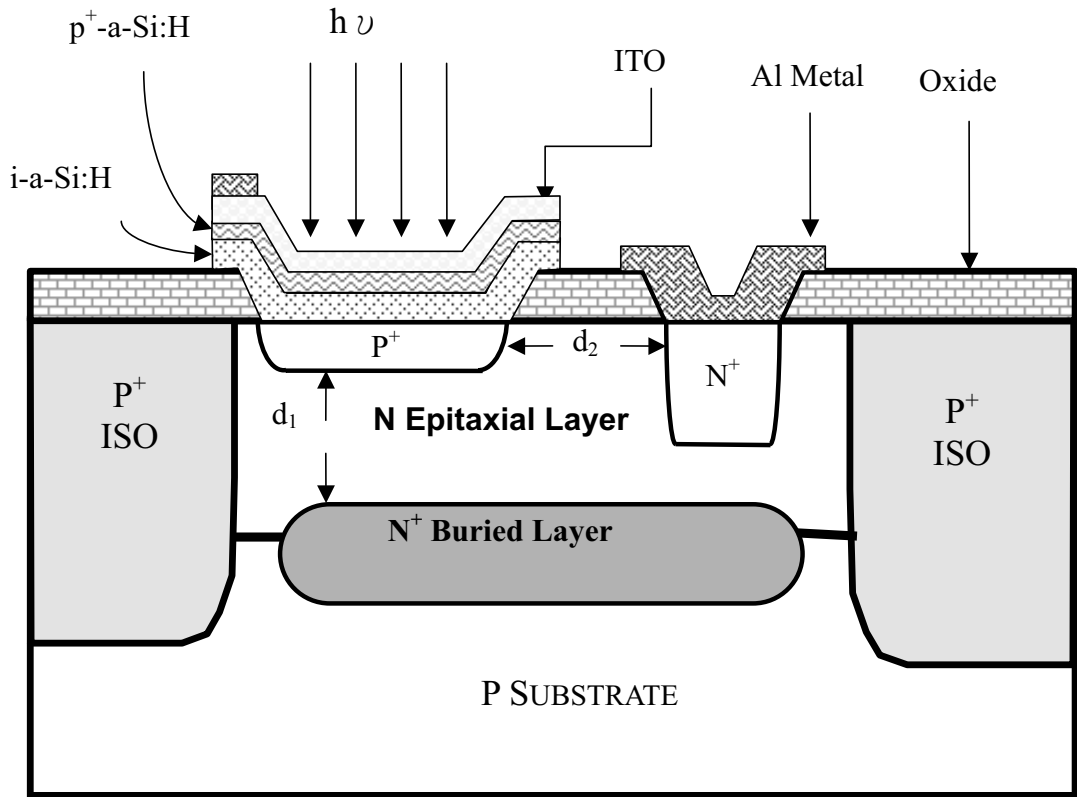


Figure 1: The schematic cross-section for proposed separated absorption multiplication region avalanche photodiodes using c-Si and/or a-Si:H materials

3. ANALYSES AND EXPERIMENTAL RESULT

APD is a specific photodiode that makes use of the avalanche phenomenon [6-7]. By adjusting the bias voltage to a level where it is on the verge of breakdown,

the photogenerated carriers can be accelerated. The accelerated carriers, in turn, produce additional carriers by collision ionization [8].

The schematic cross-section and energy-band diagram under reverse-bias for proposed separated absorption

multiplication region avalanche photodiodes using c-Si and a-Si:H materials are illustrated in Fig. 1, and Fig. 2, respectively. The fully depleted structure allows the device to be used with incident light entering the p⁺-a-Si contact to the i-a-Si region. The electron-hole pairs are photo-generated in the low-field absorption region. The photo-generated holes are swept to the p⁺-a-Si contact, while the photo-generated electrons are swept to the high-field multiplication region and are accelerated by the applied high electric field. Under high reverse-bias, the

electrons, on an average, attain sufficiently high kinetic energy larger than $1.5 E_g$ for impact ionization giving rise to secondary electron-hole pairs, where E_g the energy band gap of c-Si in the avalanche multiplication region. The secondary holes are drifted upward to the p⁺-a-Si contact, while the secondary electrons together with the initial electrons are accelerated downward to gain sufficiently high kinetic energy for impact ionization. The initial and secondary carries, in turn, generate continuously additional electron-hole pairs, which results in the avalanche current.

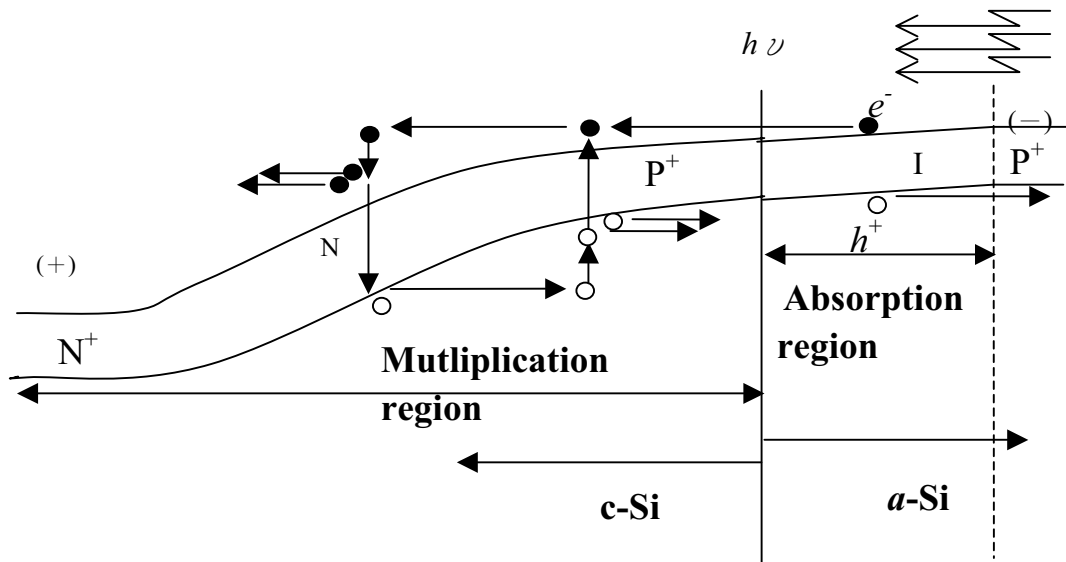


Figure 2: The schematic energy band gap diagram of the proposed device.

The light output from tungsten lamp through a monochromater (ORIEL 77200) with wavelength ranging from 200 to 1460 nm was used as the light source for measuring the photo-current and optical gain of a SAM-APD. The incident light power = 3nW with the incident wavelength

of $0.45 \mu\text{m}$ was

calibrated with an optical power meter (RIFOCS 557B). The photo-current of the SAM-APD's was measured with a semiconductor parameter analyzer (HP 4145B). Three devices with different sizes of the absorption region, i.e. the areas of of

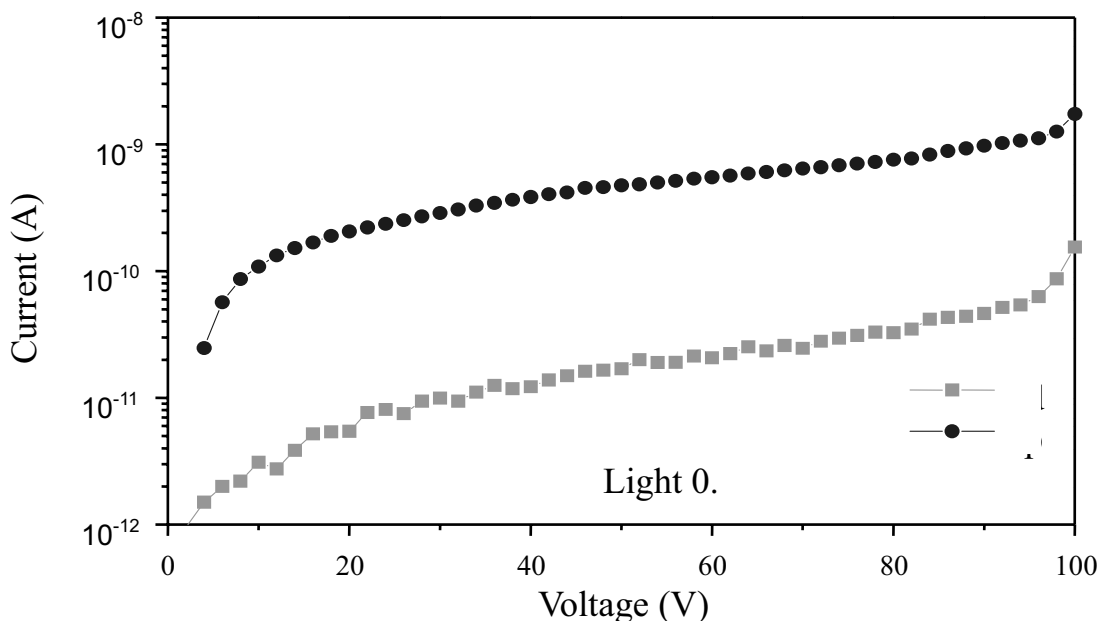


Figure 3: The photo and dark currents of device 3.

100V. Avalanche multiplication phenomenon is apparently the amorphous layer, were measured. The areas for device , 2, and 3 were $630 \mu\text{m}^2$, $528 \mu\text{m}^2$, and $434 \mu\text{m}^2$ respectively. The photo and dark currents of device.3, and optical gains of

these devices are shown in Fig. 3 and 4, respectively. The optical gain is defined as $[(I_p - I_d)/q]/(P_{in}/h\nu)$, where I_p is the photo-current, I_d is the dark current, h the plank constant, q the carrier charge, and ν the frequency of the incident light, P_{in} the

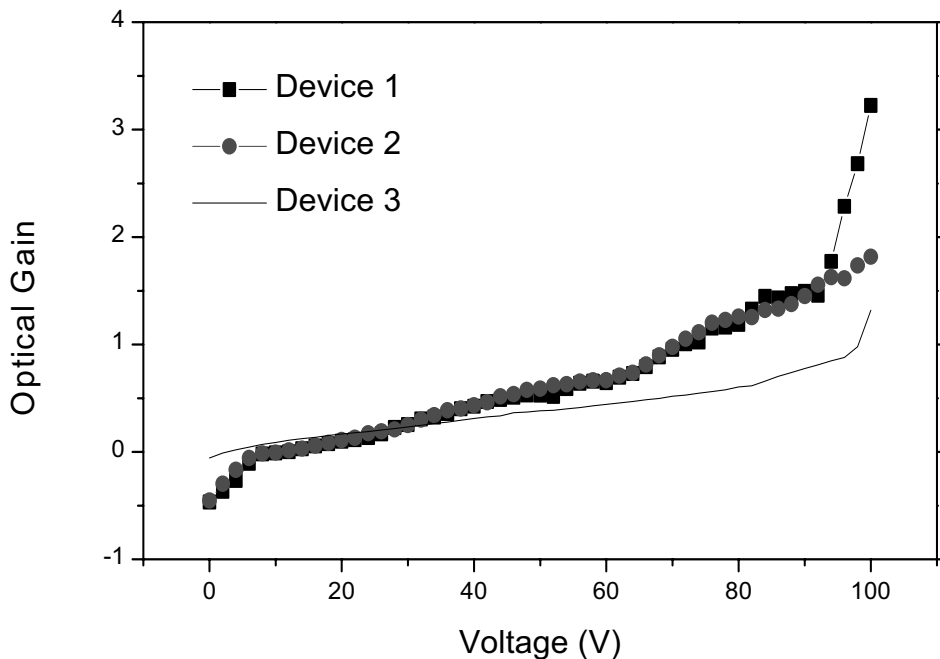
incident power. Due to the limited apply voltage of the semiconductor parameter analyzer, a maximum optical gain of 3.4 was obtained at a maximum applied voltage of 100V. Avalanche multiplication phenomenon is apparently

when the applied voltage exceeds 95V, as the rapidly increases both in photo-current and optical gain plots depicted in Fig. 3 and 4. The difference between the

experimental

4. CONCLUSIONS

The device structure of SAM-APD was expected to have high gain, low excess noise, and high absorption efficiency. However, the complexity of the fabrication process and the restrictions of measurement equipments, limits the performance of the proposed SAM-APD's. A conclusive



evaluation for the obtained SAM-APD can not be given right now. The device structure would be feasible as could be seen from the simulation results.

Figure 4: Optical gains of the proposed devices

References

[1] M. C. Teich, K. Matsuo, and B. E. A. Saleh, "Counting distributions and error probabilities for optical receivers incorporating superlattice avalanche photodiodes," *IEEE Trans. Electron Devices* **33** (1986), 1475.

[2] R. J. McIntyre, "Multiplication noise in uniform avalanche diodes," *IEEE Trans. Electron Devices* **13** (1966), 164.

[3] G. E. Bulman, V. M. Robbins, K. F. Brennan, K. Hess, and G. E. Stillman "Experimental determination of impact ionization coefficients in (100) GaAs," *IEEE Electron Device Lett.* **4** (1983), 181.

[4] K. Brennan "Theory of electron and hole impact ionization in quantum well and staircase superlattice avalanche photodiode structures," *IEEE Trans. Electron Devices* **32** (1985), 2197.

[5] Technology Modeling associates, Inc., TMA MEDICI Two- Dimensional Device Simulation Program, USA

[6] F. Capasso, "Physics of avalanche photodiodes," in Semiconductors and Semimetals, USA

[7] R. K. Willardson and A. C. Beer,

Eds. Lightwave Communications Technology, W. T. Tsang, Ed. New York:Academic, 1985, vol. 22, part D, pp. 1-172.

[8] F. Osaka, T. Mikawa and O. Wada " Electron and hole impact ionization rates in InP/Ga_{0.47}In_{0.53}As superlattice," *IEEE J. Quantum Electron.* **22** (1996), 1986.

[9] N. F. Shih "Excess Noise Analysis of Separate Absorption Multiplication Region Superlattice Avalanche Photodiodes," *IEEE Trans. Electron Devices* **48** (2001), No.6, 1705.